

DOI: 10.1002/ijch.201300081

Aldehyde–Amine Chemistry Enables Tissue Adhesive Materials to Respond to Physiologic Variation and Pathologic States

Natalie Artzi*^[a, b] and Elazer R. Edelman*^[c, d]

Abstract: Biomaterials science represents the next frontier in medical therapeutics. Innovations in materials design and formulation have helped create previously unimaginable interventions and composite devices with materials whose structure and function evolve with time. Yet, materials development has outstripped our ability to explain why, when, and how these materials work. Current characterization means are limited, especially for dynamic erodible materials that are specifically designed to fade away. This complexity and dynamism of emerging materials and the impact they have on tissue make it challenging to understand and predict material interactions with local tissues. Because tissue–biomaterials interactions are determined not only by the innate properties of the materials, but also by the local microenvironment at the implantation site, we must now examine the impact of target tissue site, state, and incidence of a disease on material performance, efficacy, and biocompatibility. This issue becomes increasingly important when considering surface interacting materials, whose intimate interactions with tissues are dictated by local mechanical

forces, tissue target site, and the modulation of tissue surface properties manifested by specific disease types and states. The mechanisms involved and the extent to which these parameters affect the in vivo performance of materials are mostly unknown. These open questions motivated us to explore the determinant factors that affect the efficacy of materials, using adhesive materials whose surface interactions with tissues make them an ideal material class for the assessment of tissue–material interactions. As an example of this paradigm, we determined how tissue amines served as a natural binding site for material aldehydes, enabling tissue-specific binding that varied with natural changes in amine density from tissue to tissue and the physiologic environment, as well as with disease. The introduction of amines within the material also provides greater control over binding and material cohesion. This general mode will provide new tissue adhesives that can sense local tissue states and provide mechanical interactions titrated to context and need to enhance the desired effect and minimize local toxicity.

Keywords: aldehydes · amines · biomaterials · medicinal chemistry · polymers

1 Introduction

Materials that undergo regulated dimensional change may well serve as a new class of therapeutic devices; in particular, materials designed for site-specific surface interfaces with predictably modulatable functionality and induced responsiveness. Materials with specific properties matched to the mechanical and surface properties of target tissues can, for example, be used to augment wound closure typically achieved with sutures or staples, repair of surface lacerations and abrasions of solid organs, sustained and localized drug delivery, and structural reinforcement of void tissue spaces. In all adhesive material indications, appropriate mechanical properties of the applied material are essential for therapeutic benefit and lack of toxicity. Current adhesive materials are however limited and active questions and limitations force physicians to choose between extremes of adhesion strength and biocompatibility.^[1] As an example, common cyanoacrylate derivatives adhere strongly to tissue, but their vigorous and uncontrolled tissue cross-linking along with the release of toxic degradation byproducts dramati-

-
- [a] N. Artzi
Institute for Medical Engineering and Science
Massachusetts Institute of Technology
E25-449, 77 Massachusetts Ave.
Cambridge, MA 02139 (USA)
fax: +1 (617)253-2514
e-mail: nartzi@mit.edu
- [b] N. Artzi
Department of Anesthesiology
Brigham and Women's Hospital
Harvard Medical School
Boston, MA 02115 (USA)
- [c] E. R. Edelman
Thomas D. and Virginia W. Cabot Professor of Health Sciences
and Technology
Massachusetts Institute of Technology, E25-449
77 Massachusetts Ave.
Cambridge, MA 02139 (USA)
fax: +1 (617)253-2514
e-mail: ere@mit.edu
- [d] E. R. Edelman
Cardiovascular Division, Department of Medicine
Brigham and Women's Hospital
Harvard Medical School
Boston, MA 02115 (USA)

cally impedes healing and regeneration processes.^[2–4] Although sealants rely on intimate tissue–material interactions for functional adhesion, target-tissue properties have been largely ignored in material design. Instead, one general formulation is proposed for application to the full range of soft tissues across diverse clinical applications.^[5–10] This article brings examples of the factors affecting tissue–material interactions and how tissue micro-environments should be exploited for the rational design of materials to achieve desired clinical outcomes.

2 Mechanical Loads Associated with Target Organs Dictate Material Mode of Failure

Adhesive material failure falls into two complementary domains: loss of adhesion and/or cohesion. The former involves the inadequacy of secured interaction between material and tissue and the latter involves the insufficiency of internal material integrity. This much is well established, but what is becoming increasingly appreciated is that each tissue and application environment presents unique targets and demands on biomaterials, and thus, the principles and approaches toward tissue- and application-specific materials design are of growing interest.^[11] Soft-tissue adhesive materials are employed to repair and seal many different organs, which range in tissue surface chemistry and in mechanical challenges during organ function. This complexity motivates the development of tunable adhesive materials with high resistance to loss of either adhesive security or cohesive integrity under uni- or multiaxial loads dictated by a specific organ environment.

Most of the tissue adhesives utilize aldehyde functional materials binding to tissue amines. This is the mechanism of action of tissue cross-linking fixatives such as glutaraldehyde and formaldehyde and for clinical adhesives such as GRF glue (gelatin–resorcinol formaldehyde) as well.^[12] The low viscosity, low-molecular-weight aldehyde solutions penetrate deep into the tissues and react with tissue amines to create tight bonds but not without a price. The degree of cross-linking and tight spacing of the aldehydes impairs tissue mobility and pliability, and any excess free aldehydes are toxic to the tissues. In addition, the heat generated during the cyanoacrylate reaction with tissues devitalized several layers of cells.

The PEG–dextran family of materials provides the ideal system for addressing these issues and studying these processes. Copolymeric hydrogels comprising aminated star polyethylene glycol and dextran aldehyde (PEG–dextran) are adhesive materials^[13] that create a material with a network of flexible arms to retain the aldehyde linkers and internal amines to sop up the excess aldehydes. Such a copolymeric system offers independent modification of the solid content and molecular weight of each of the PEG and dextran components, the degree of

aldehyde oxidation, and the number of arms in the stellate PEG to create materials with the full spectrum of material properties and material–tissue interactions. The network of PEG–dextran is first formed through binding between aldehydes and amines to assure cohesion (Figure 1a). Those aldehydes that are still free remain reactive, such that adhesive bonds can form between this network and opposing amines of adjacent tissues. The usual excess of aldehydes that can give rise to a toxic tissue response is attenuated by the internal amines. In this way, adhesion can be attained with minimal effect on material pliability, and free aldehyde toxicity can be reduced by internal immobilization of internal polymeric amines forming imine bonds. This latter feature adds to cohesive integrity. As internalized aldehydes bind material the cohesion of amines rises, creating a material whose adhesion and cohesion are titrated to tissue content and state. Identification of design parameters that optimize adhesion while minimizing adverse tissue response requires efficient characterization of the materials at complex interfaces, such that, for example, the aldehyde content is carefully titrated to support cohesion and adhesion based on tissue needs.

The multiple components of this PEG–dextran network and their independence provides not only a flexible and dynamic material, but a model system for examining chemically directed material interactions with external targets and internal structures as well. This material and its modification potential enable us to examine aspects of material–tissue interactions with greater precision than ever before. Because material aldehydes react with tissue amines, we can now quantify the adhesion of a material to a target tissue by assaying for the force required to part the paired components of the amine reaction sites on the tissue and material aldehydes.^[11–13] We examined the impact of different components on adhesive binding and cohesive material integrity. AFM probes were functionalized^[12] with amine groups to represent the tissue surface functionality (Figure 1b). We used these probes to define the unbinding force from the PEG–dextran adhesives as a metric of the binding or interaction potential of these adhesives to tissues exhibiting a range of amine-reactive groups. Mechanical testers directly measured adhesive material performance and compared these two length scales. Interestingly, AFM-enabled force spectroscopy (Figure 1b) and macroscale tissue–adhesive–tissue rupture experiments (Figure 1c) approximate a uniaxial tensile stress state at the interface, and hence, these failure loads were well correlated. In contrast, the tissue samples subject to pressure rising to burst threshold are subject to a more complex, multiaxial stress state of forces (Figure 1d).

Thus, aldehydes bind amines internally for cohesive integrity and externally for adhesive security. Yet, the balance between adhesion and cohesion and relationship with composition is not straightforward: it must take into

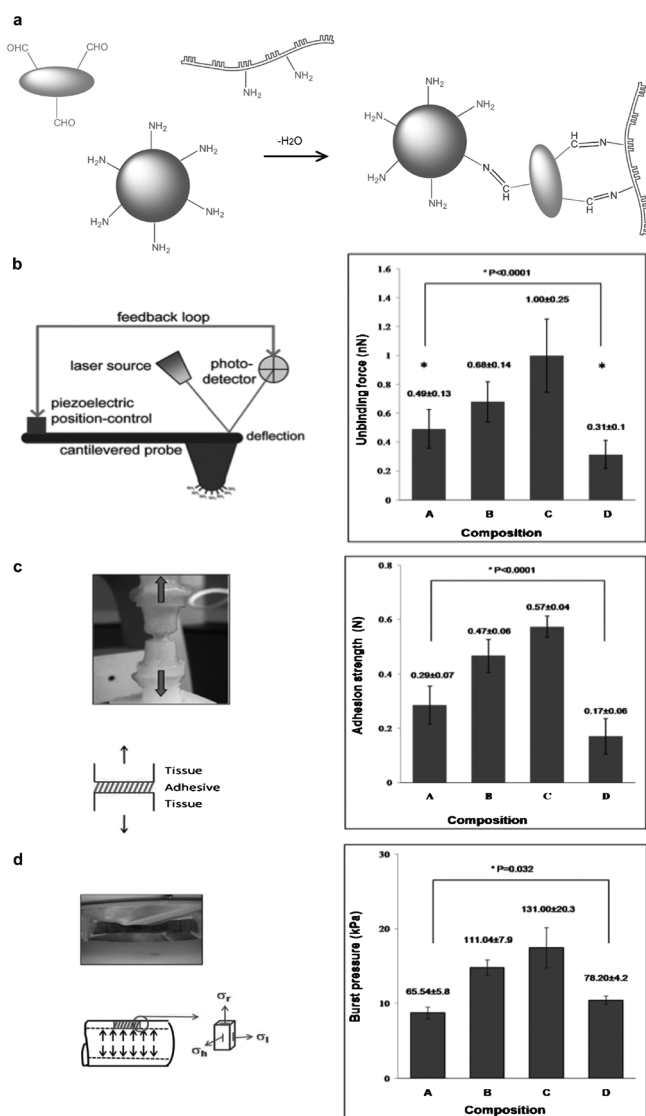


Figure 1. a) Schiff base reaction between polymers based on PEG–amine and dextran aldehyde provides material cohesion, while the dextran aldehyde reaction with tissue amines supports material adhesion to tissue surfaces. b) An amine-functionalized AFM tip, mimicking tissue surfaces, is used to quantify the potential interaction of tissue amines with material aldehydes, providing a measure of the unbinding force required to separate the two. Four compositions differing in dextran aldehyde solid content (compositions A–C, with 8.75, 14, and 18 wt% dextran aldehyde, respectively, 50% oxidation), and with lower aldehyde density while having the same total amount of aldehyde groups (composition D, 23 wt% dextran aldehyde and 20% oxidation). c) Adhesion strength of compositions A–D applied to a rat small intestine in uniaxial tensile loading (values reported as average \pm standard deviation). d) Burst pressure of compositions A–D applied to a rat small intestine (values reported as average \pm standard deviation). Stresses within and at the interface are multiaxial, including interfacial shear as well as radial, longitudinal, and hoop stresses σ_r , σ_l , and σ_{hr} , respectively.

account tissue target density as well. There is not an infinite number of aldehyde–amine pairs and even when not

saturated there are densities of either component that are arrayed suboptimally for interaction. Here, steric hindrance dominates. It is not sufficient to have an abundance of aldehydes, but rather the aldehydes must be aligned for optimal interaction with the target amines. Thus, unbinding force, adhesive strength, and burst pressure increase with aldehyde content (Figure 1b–d), but compositions featuring low aldehyde density can establish a higher macroscopic burst pressure under the triaxial stress state if aldehyde–amine steric interactions are optimized. This in turn led to different modes of failure, supporting adhesive failure in uniaxial stress and cohesive failure when triaxial stress was applied. Triaxial stress is most representative of perfused organs such as the small intestine and can be greater for compositions with more effective aldehyde spacing. Cohesive strength may be lost, which somewhat demonstrates the independent control of specific parameters with this formulation (Figure 1d).

By comparing the failure modes (adhesive vs. cohesive) and effects of compositions (number vs. density of aldehyde groups) among three mechanical characterization approaches, we inferred the extent to which dextran aldehydes react with PEG amines (within the adhesive material) versus tissue amines (at the tissue–adhesive interface). Our experiments demonstrate that the distribution of aldehyde groups along the exposed chains plays a key role in adhesion to these tissues for the practical application of interest: sealing of open serosal wounds of the small intestine subjected to perfusion pressure. Thus, adhesive materials for in vivo use require that macroscale experiments reflect the mechanical loading states anticipated for wound sealing applications in vivo. AFM can characterize the aldehyde density of the material available for tissue interaction and in this way enable rapid, informed material choice. Further, the correlation between AFM quantification of nanoscale unbinding forces with macroscale measurements of adhesion strength by uniaxial tension or multiaxial burst pressure allows the design of materials with specific cohesion and adhesion strengths.

3 Effect of Tissue–Material Interactions on Material Fate and Means to Predict In Vivo Retention Time

The extent of tissue–material interactions should largely determine the tissue retention of adhesive materials. However, degradation in vivo is more complex than that in vitro, and in vitro assays are rarely adequate measures of implant behavior.^[14] Loss of material integrity, structure, and eventually mass, progress dependently over time, but are dominated by different environmental forces in vitro and in vivo. The question remains as to whether erosion or loss of mass in one domain can pre-

dict performance in the other. Gravimetric determinations from periodic sampling of explant weight cannot follow the same sample over time, necessitate a large number of animals to follow a small number of samples, and have excessive variability. Chromatography tracks molecular weight changes, but cannot be applied to eliminable materials that do not undergo chain scission and retain their molecular weight. Material environment affects erosion, and the material and degradation products may affect the environment in turn. Thus, in vivo residence times and in vitro durability of three-dimensional degradable structures differ. We developed a noninvasive imaging technique that tracked material erosion in vivo through a fluorescent tag covalently attached to components of model materials. Material erosion was calculated from the decay in total material fluorescence signal using a noninvasive in vivo imaging system (IVIS). Fluorescent PEG–dextran materials were submerged in media under

defined conditions. The presence of released fluorescent signal was monitored as the media were periodically changed. This signal is a surrogate for the effective material loss from a tissue surface and varied based on underlying tissue type. Formulation protocols control erosion profiles because network formation dictates fluid uptake and depends on the aldehyde/amine ratio. PEG amine solid content affects cross-linking density, and hence, degradation kinetics (Figure 2a). We used mathematical modeling to fit each data set to a dual exponential decay model, shedding light on the erosion mechanism. In this model, polymer mass, M , follows the erosion of two components, each defined by the relative proportion of total mass, and a specific erosive rate constant, k , at each phase (Figure 2b). The relationships between the total mass and erosive rate constant at each phase (Figure 2c) can be used to interpolate the values for new formulations and predict their in vitro erosion kinetics (Fig-

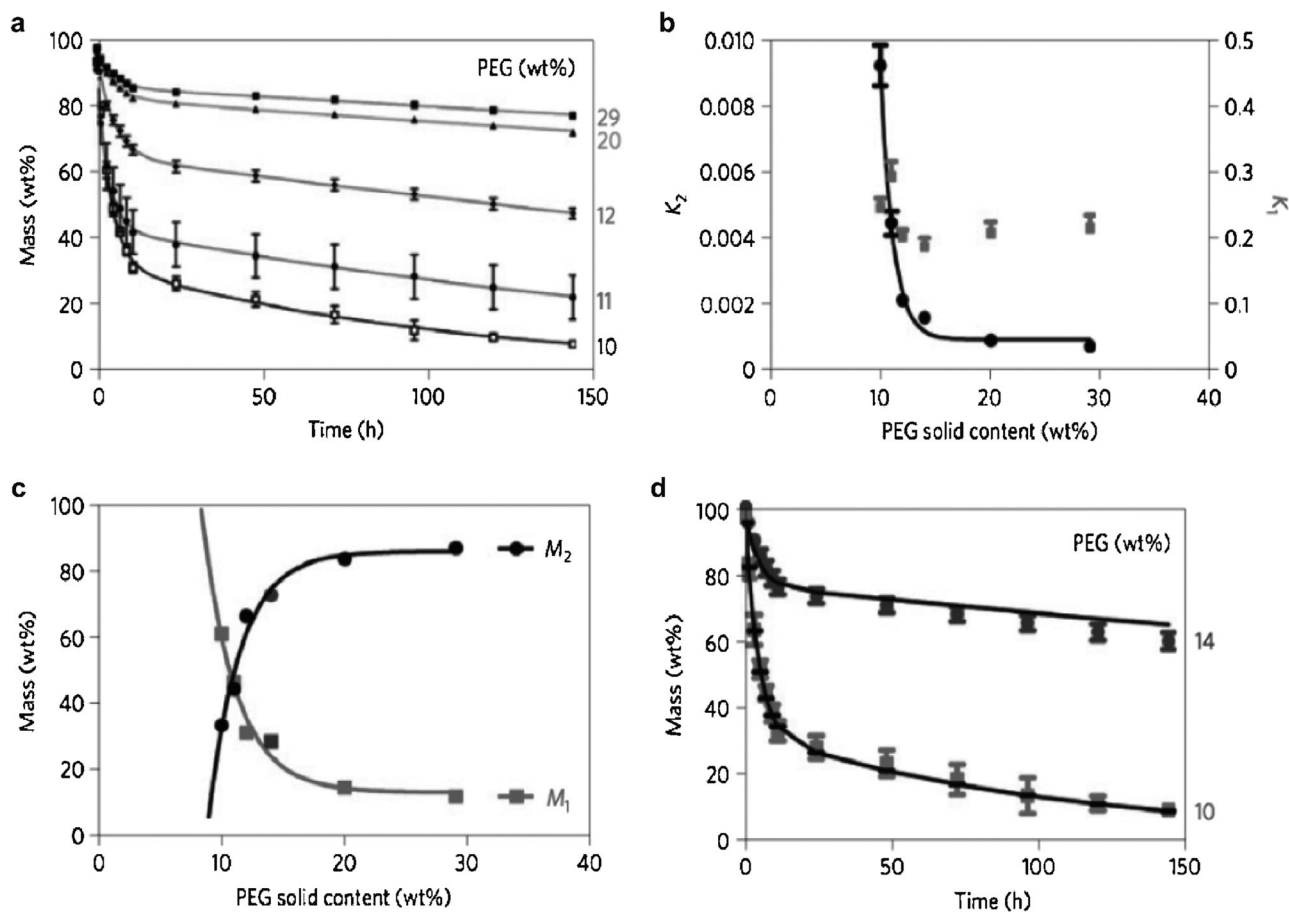


Figure 2. a) Alteration of PEG solid content from 10 to 29 wt% enables fine-tuning of material erosion kinetics. Model descriptors are presented as a function of PEG solid content. b) and c) Whereas k_1 is constant and k_2 decays exponentially (c), M_1 and M_2 similarly demonstrate reciprocal exponential changes with PEG solid content. The relationships between model descriptors and PEG solid content (PEG_{SC}) are as follows: $k_2 = 53.7 \exp[-0.88(\text{PEG}_{\text{SC}})] + 0.0009$, $M_1 = 3.979 \exp[-0.44(\text{PEG}_{\text{SC}})] + 12.4$, and $M_2 = -3.028[1 - \exp[-0.41(\text{PEG}_{\text{SC}})] + 85.4]$. d) Using the equations describing the relationship between model descriptors and PEG solid content, the erosion profile of new compositions containing 10 and 14 wt% PEG were prospectively predicted (points are empirically accumulated and lines are model predictions). Constants were extrapolated from the data fits and are inserted as blue symbols; squares represent k_1 and M_1 , and circles represent k_2 and M_2 . Predicted erosion correlated well with empirical observations (Pearson's coefficient $R = 0.99$).

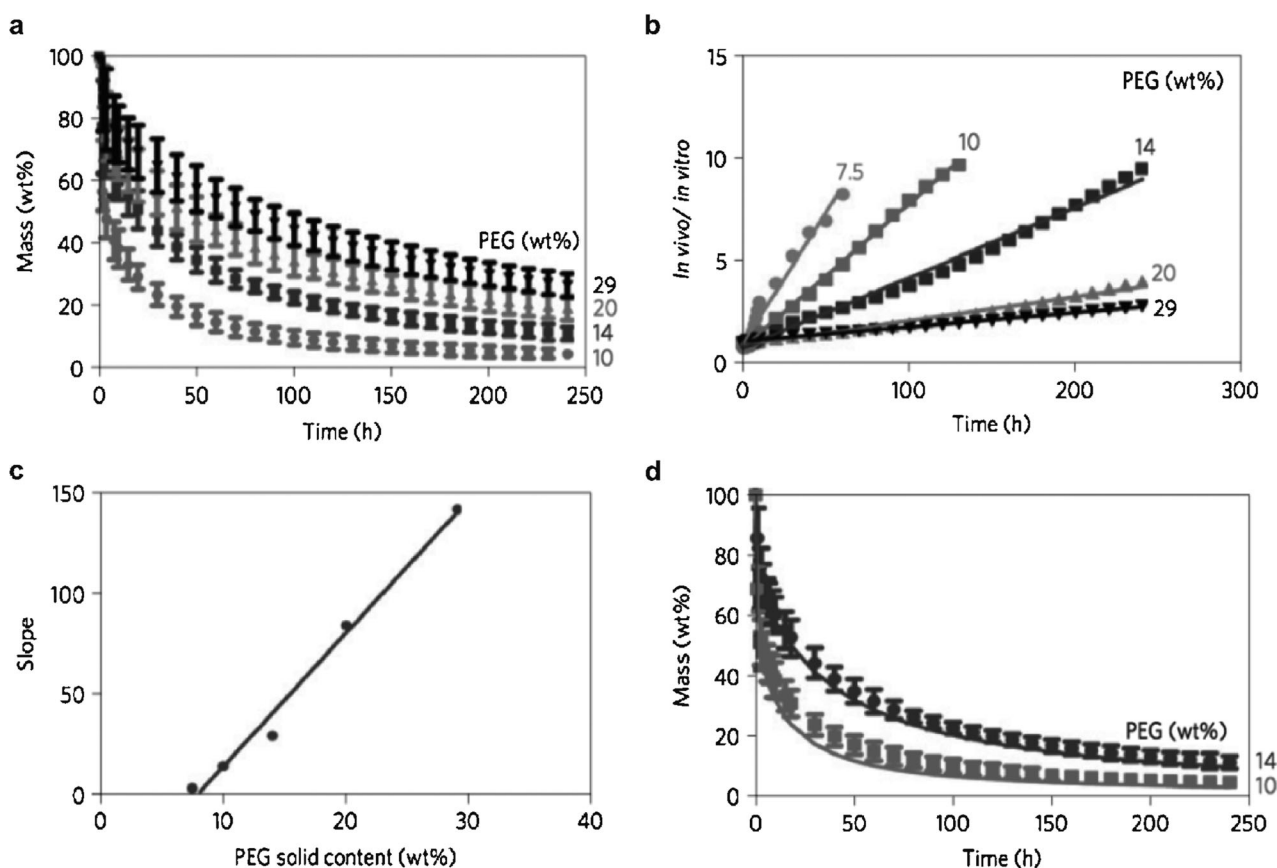


Figure 3. a) In vivo erosion of PEG–dextran formulations is depicted and follows the trend of the in vitro erosion profile, at a faster pace, as demonstrated for compositions with 10, 14, 20, or 29 wt% PEG solid content. b) A linear relationship exists between the ratio of in vivo and in vitro erosion as a function of time for all PEG solid contents examined. c) The slopes of these curves linearly correlate with PEG solid content. d) Using this linear relationship, in vivo erosion profiles of two different formulations were accurately predicted from in vitro data ($R=0.99$; points are empirically accumulated and lines are model predictions).

ure 2d). However, the greatest benefit of such a model is the ability to predict in vivo erosion kinetics of newly synthesized materials from in vitro data by finding the relationships between in vitro (Figure 2a) and in vivo erosion (Figure 3a) of known formulations, as successfully performed for materials with varied PEG formulations. The slope of the graph featuring the ratio between in vivo and in vitro erosion plotted versus PEG solid content (Figure 3b and c) was linear, enabling simple calculation of in vivo erosion of a newly synthesized composition from its in vitro data successfully (Figure 3d). This practice helps minimize the number of animals used and also serves as a convenient material-screening platform in vitro. Exploiting optical imaging in vitro and in vivo facilitates the examination of one factor at a time in a controlled in vitro environment while seeking for correlative in vivo behavior. The existence of a correlation between the two domains would inform us under what conditions the in vitro governed processes were clinically relevant, and hence, predictive of the in vivo performance. Such a procedure would enable the design of materials that could

perform specific functions with predictable properties for specific medical applications.

4 Impact of Target Organ Site on Tissue–Biomaterial Interactions

Until now, we have assumed that only the material changes and that the six degrees of freedom in the PEG–dextran adhesive network create a significantly expansive opportunity for tissue tunable materials. Yet, it is the tissue that has the greatest potential for variation and gradation, across a virtually infinite spectrum of states. Each tissue has a different structure, composition, and density of binding sites and each physiologic state and pathologic stress imposes changes that range from subtle to profound. Tissue responsive materials should match each state to avoid loss of adhesion and gain of toxicity. Recall that local inflammation and general tissue toxicity are also related to material aldehyde density.^[12] These concepts define a therapeutic window for optimal tissue–sealant interactions, bounded below by the need for ade-

quate adhesion strength and above by the condition of biocompatibility.

To examine this balance, adhesive mechanics were measured in a range of organs, including the heart, lung, liver, and duodenum. Tissues were harvested from rats immediately after animal sacrifice and biopsy specimens of uniform thickness and surface area were accumulated to facilitate uniaxial mechanical testing of tissue–material interfaces.^[11] Tissue biopsies were reacted with aldehyde-coated fluorescent microspheres (f-MS) through gentle mixing in an aqueous solution. Following suspension, the fluorescent intensity at the surface of the tissue samples was quantified to generate an aldehyde conjugation metric reflecting the percent of tissue-surface coverage by immobilized f-MS (Figure 4a). The conjugation metric is indicative of the aldehyde affinity of soft tissues, and provides a fairly direct measure of the targeted biochemistry for PEG–dextran adhesion. Soft tissues display a range of f-MS conjugation metrics, with duodenal tissue possessing the greatest apparent aldehyde affinity. Comparison of tissue-conjugation metrics to adhesive mechanical data provides convincing evidence for aldehyde-mediated adhesion because interfacial moduli strongly correlate ($R=0.92$, $p<0.05$) to aldehyde affinity across the tested tissue types and material variants. The aldehyde content of materials and aldehyde affinity of tissue seemingly present a mechanism by which to design and select materials based on clinical applications.

The interfacial regions between PEG–dextran and excised rat heart, lung, liver, and duodenum tissues were microscopically examined to add physical insight to adhesive interactions. The same material formulation conjugated differentially with the four different tissues (Figure 4a) and exhibited different patterns of adhesion and cohesion (Figure 4b). Three distinct domains were evident upon material adherence, including the target tissue, bulk material, and an adhesive regime interposed between the two (Figure 4b). The adhesive force of interaction with the tissue and interfacial patterns tracked with density of amines within the tissues. The adhesive regime depicts the intermediate material structure resulting from concurrent dextran aldehyde reactivity with PEG and tissue amines. The morphology of the adhesive regime varied with tissue type, primarily through the different density of surface amines available to the aldehydes, appearing fibrillar and discontinuous on cardiac and lung tissues, and more continuous and intact over liver and duodenum. Adhesive interactions then in turn created different internal structures as material amines were increasingly bound to aldehydes not interacting with tissue targets.

The benefit of increased adhesion of materials with greater aldehyde content must be balanced by adverse biologic responses to excess free aldehydes. Substantial differences in soft-tissue aldehyde affinity shift the balance between adhesion and inflammation for each tissue, and

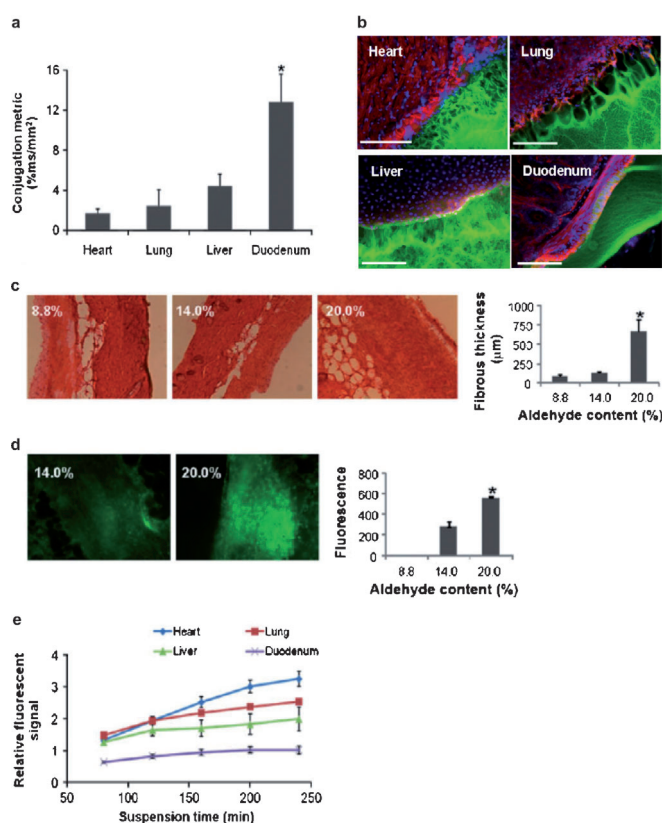


Figure 4. a) The relative aldehyde reactivity of heart, lung, liver, and duodenal rat tissue were assessed through tissue-sample conjugation of fluorescent aldehyde-coated microspheres. Aldehyde reactivity was lowest in the lung and heart, greater in the liver, and highest in the duodenum (* $p < 0.05$ compared with liver and duodenum). b) The interface between PEG–dextran (green) and various soft tissues, highlighted with rhodamine phalloidin (actin, red) and DAPI (cell nuclei, blue), varies with tissue. c) Tissue reactivity in vivo was assessed for subcutaneous implants of materials with low (8.8 wt%), medium (14.0 wt%), or high (20.0 wt%) dextran aldehyde solid content. A subcutaneous pocket was created in anesthetized C57BL/6 mice and 200 μ L of material was injected into the pocket using a syringe with a mixing tip. After nine days, the mice were sacrificed and the skin and subcutaneous tissue were harvested. The samples were snap frozen in liquid nitrogen and stored at -80°C until histological and zymographic analysis. Materials with increased aldehyde content cause an increased inflammatory response. Histomorphometric analysis reveals increased fibrotic capsule thickness and inflammatory cell present in materials with a high aldehyde content. d) Gelatinase zymographic activity was increased with material aldehyde levels. (* $p < 0.05$ compared with 14.0% solid content). e) Differential adhesive retention was seen when applied to different tissues. Adhesive is most stable when applied to the duodenum, while those applied to the liver, lung, and heart degrade faster and at an increasing rate. Degradation rate correlates with material affinity to the tissues ($R=0.9$, $p < 0.05$).

suggest that a class of materials could be optimized for specific needs. Excess aldehydes might simply be minimized when tissues are less responsive to changes in material aldehyde content, as in the case of lung tissue. In the other tissues, where aldehyde affinity is higher and re-

sultant adhesion increases, the intense response to material chemistry allows one to consider designing compositions for anticipated duration and desired strength of adhesion. Although tissue-surface chemistry is often ignored, it is a critical determinant of tissue-material interaction.

The *in vivo* biocompatibility of PEG–dextran materials and influence of material aldehyde content on tissue response was evaluated in subcutaneous material implants. PEG–dextran variants with dextran aldehyde solid content over a wide range were implanted into a subcutaneous pocket in mice that survived for nine days. Inflammation, as manifested by a thicker fibrous capsule, increased with aldehyde content (Figure 4c). Inflammatory cell-mediated proteolysis affects wound repair as matrix metalloproteases cleave the extracellular matrix, weakening the tissue and surgical anastomoses. The gelatinase activity in the tissues, measured using analytical fluorescent microscopy and *in situ* zymography, also increased with material aldehyde content (Figure 4d). This trend in proteolytic activity is likely to be a result of the increased pro-inflammatory mediators and activation of polymorphonuclear leukocytes generated by the reactive aldehyde groups.

We have already shown that the extent of tissue-material interactions with a specific tissue surface supported by different PEG–dextran formulations largely deter-

mines *in vivo* tissue retention of the adhesive materials. Then we examined what the impact on degradation would be when the same adhesive formulation was applied to different tissue types. Material was applied to different tissue biopsies and submerged in media. The loss of fluorescence with time and its accumulation in the media was used to track degradation. Interestingly, the differential extents of interaction with the different organs supported relatively rapid fluorescent accumulation when PEG–dextran was applied to heart and lung tissue, indicating fast degradation, while hepatic and duodenal specimens exhibited protracted degradation kinetics (Figure 4e). The divergence in retention time attained when the same material formulation was applied to different tissues reiterated the importance of examining materials in light of their clinical use.

5 Impact of Disease on Material Efficacy and the Associated Biological Response

The full spectrum of biomaterial interactions can only be appreciated in the setting of disease, where the greatest dynamism in target tissue microenvironment and tissue ultrastructure is evident. We investigated the effect of inflammatory (colitis) and neoplastic (colorectal cancer) bowel diseases on tissue properties and tissue–material

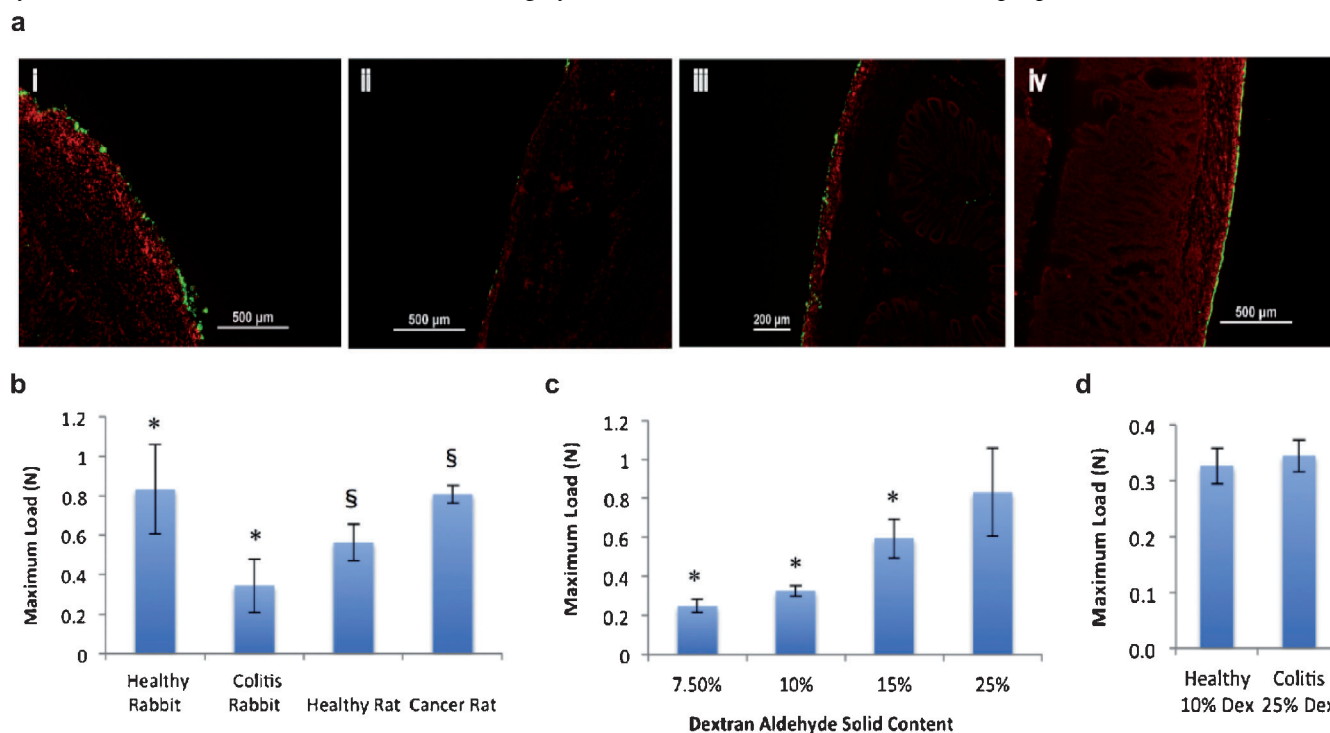


Figure 5. a) Tissue–material interactions as a function of disease type was assessed by quantifying amine density on colon serosal layer using aldehyde-coated f-MS (green) in healthy rabbit (i) and inflamed (ii) tissues and healthy rat (iii) and neoplastic (iv) tissues (red, stained with propidium iodide). b) Maximum load at failure is depicted for all tissue types and c) for different material formulations (dextran aldehyde solid contents from 7.5 to 25% with fixed dendrimer amine solid content of 20%) on healthy rabbit colon. Dextran aldehyde solid content can be tuned to match the surface amine density of the target tissue. d) By increasing the dextran aldehyde solid content from 10 to 25%, statistically equal levels of adhesion can be achieved in healthy and inflamed tissues, respectively.

interactions. These processes span the range of tissue responses and indeed amine presentation when tissue surface chemistry was evaluated using aldehyde-coated microspheres conjugation. While colitis reduced surface amine density (Figure 5a–ii vs. i, b), as seen by the lower conjugation of aldehyde-coated microspheres, colorectal cancer raised surface amine density (Figure 5a–iv vs. iii, b). These results correlated with the macroscopic measurement of adhesion failure, as measured by using a mechanical tester while recording the maximum applied tensile load at failure. Load-to-failure decreased 58% in the case of colitis and increased 43% for colorectal cancer. The significant reduction in adhesion in the case of colitis tissue can lead to loss of adhesion soon after material implantation that cannot be foreseen if the material is only applied to a healthy tissue, creating a stable bond. This demonstrates the importance of optimizing materials for specific clinical scenarios.

Material formulation can be altered to match different clinical scenarios (Figure 5c). As dextran aldehyde solid content increased from 7.5 to 25 wt%, maximal load at failure increased by 235%. This flexibility in material design can be utilized to enhance adhesion in the case of colitis, where fewer amine groups are available for interaction with the material. Hence, excess aldehydes provided by means of higher dextran aldehyde solid content would increase the probability for material interactions with tissue amines. Interestingly, by increasing the dextran aldehyde solid content from 10 wt% in healthy tissue to 25 wt% in the case of colitis, we were able to compensate for the reduction in tissue amine density in the disease state and achieve the same level of adhesion strength as in the healthy state (Figure 5d).

6 Summary and Outlook

Material performance, tissue–material interactions, and thus, therapeutic outcomes are contextual. Hence, it is critical to assess tissue microenvironments and develop materials in the settings of clinically relevant conditions to enable predictable and favorable material performance. Polymeric materials designed as adhesives for biological applications require optimization of interfacial failure resistance, degradation rates, and biocompatibility in light of their intended use. We demonstrated that material integrity and adhesion to local tissues depended on environmental factors and was not only a constitutive property of the material. Characterization of failure in the macroscale should mimic the local mechanical loading profile. Uniaxial load requires sealant materials with high

cohesive strength, whereas when sealants are subject to multiaxial load adhesive strength becomes more dominant. Additionally, target organ sites give rise to variable surface chemistries, dictating the resulting adhesion strength. Material formulation should consider these changes in the design stage to prevent unforeseen outcomes in preclinical settings. Finally, disease modifies tissue surface chemistry in a disease-specific manner and requires careful titration of materials to specific indications. The ability to design responsive materials coupled with the growing understanding of the impact of tissue microenvironments on the performance of materials calls for new approaches for the design and characterization of materials in a setting that will support the development of preclinical models, which can be subsequently extrapolated to predict characteristics in patients.

References

- [1] M. Araki, H. Tao, N. Nakajima, H. Sugai, T. Sato, S.-H. Hyon, T. Nagayasu, T. Nakamura, *J. Thorac. Cardiovasc. Surg.* **2007**, *134*, 1241–1248.
- [2] A. Ekelund, O. S. Nilsson, *International Orthopaedics* **1991**, *15*, 331–334.
- [3] C. Vauthier, C. Dubernet, E. Fattal, H. Pinto-Alphandary, P. Couvreur, *Adv. Drug Delivery Rev.* **2003**, *55*, 519–548.
- [4] B. J. Vote, M. J. Elder, *Clin. Exp. Ophthalmol.* **2000**, *28*, 437–442.
- [5] M. Serra-Mitjans, J. Belda-Sanchis, R. Rami-Porta, *Cochrane Database Syst. Rev.* **2005**, CD003051.
- [6] M. Scotté, F. Dujardin, A. Amelot, P. Azema, I. Leblanc, P. Bouvier, F. Michot, P. Ténrière, *Eur. Surg. Res.* **1996**, *28*, 436–439.
- [7] R. Rami, M. Mateu, *Cochrane Database Syst. Rev.* **2001**, CD003051.
- [8] D. Mutter, M. Aprahamian, C. Damge, P. Sonzini, J. Marescaux, *Biomaterials* **1996**, *17*, 1411–1415.
- [9] E. Lim, P. Goldstraw, *Eur. J. Cardiothorac. Surg.* **2007**, *32*, 552–553.
- [10] M. Kawamura, M. Gika, Y. Izumi, H. Horinouchi, N. Shinya, M. Mukai, K. Kobayashi, *Eur. J. Cardiothorac. Surg.* **2005**, *28*, 39–42.
- [11] N. Artzi, T. Shazly, A. B. Baker, A. Bon, E. R. Edelman, *Adv. Mater.* **2009**, *21*, 3399–3403.
- [12] C. H. Fox, F. B. Johnson, J. Whiting, P. P. Roller, *J. Histochem. Cytochem.* **1985**, *33*, 845–853.
- [13] N. Artzi, A. Zeiger, F. Boehning, A. bon Ramos, K. Van Vliet, E. R. Edelman, *Acta Biomater.* **2011**, *7*, 67–74.
- [14] N. Artzi, N. Oliva, C. Puron, S. Shitreet, S. Artzi, A. bon Ramos, A. Groothuis, G. Sahagian, E. R. Edelman, *Nat. Mater.* **2011**, *10*, 704–709.

Received: July 14, 2013
Accepted: August 29, 2013